Article

Modeling di (2-ethylhexyl) Phthalate (DEHP) and Its Metabolism in a Body's Organs and Tissues through Different Intake Pathways into Human Body

Ao Li, Lingyi Kang, Runjie Li, Sijing Wu, Ke Liu and Xinke Wang *

School of Human Settlements and Civil Engineering, Xi'an Jiaotong University, Xi'an 710049, China;
kichelle620@163.com (A.L.); kanglingyi123@163.com (L.K.); lirunjie@stu.xjtu.edu.cn (R.L.);
wsj13572050386@163.com (S.W.); mjyrke95@163.com (K.L.)
* Correspondence: wangxinke@mail.xjtu.edu.cn

Abstract: Phthalate esters (PAEs) are ubiquitous in indoor environments as plasticizers in indoor products. Residences are often exposed to indoor PAEs in the form of gas, particles, settled dust, and surface phases. To reveal the mechanism behind the accumulation of PAEs in different tissues or organs such as the liver and the lungs when a person exposed to indoor PAEs with different phases, a whole-body physiologically based pharmacokinetic model for PAEs is employed to characterize the dynamic process of phthalates by different intake pathways, including oral digestion, dermal adsorption, and inhalation. Among three different intake pathways, dermal penetration distributed the greatest accumulation of DEHP in most of the organs, while the accumulative concentration through oral ingestion was an order of magnitude lower than the other two doses. Based on the estimated parameters, the variation of di-ethylhexyl phthalate (DEHP) and mono (2-ethylhexyl) phthalate (MEHP) concentration in the venous blood, urine, the liver, the thymus, the pancreas, the spleen, the lungs, the brain, the heart, and the kidney for different intake scenarios was simulated. The simulated results showed a different accumulation profile of DEHP and MEHP in different organs and tissues and demonstrated that the different intake pathways will result in different accumulation distributions of DEHP and MEHP in organs and tissues and may lead to different detrimental health outcomes.

Keywords: exposure; indoor; metabolism; PBPK model; phthalate esters

1. Introduction

Phthalate esters (PAEs), a kind of semi-volatile organic compound, have been widely used as plasticizers in household and industrial products for decades, primarily to increase the flexibility and resilience of polyvinyl chloride (PVC) products. Since they are not chemically bounded to a product matrix, PAEs will be gradually released from indoor products into the air and tend to adhere to suspended particulate matter, dust, and indoor surfaces because of their low vapor pressure. Thus, PAEs have been detected in almost all indoor environments [1–6], and exposure to indoor PAEs seems especially severe in China [7,8]. What is more, during the on-going COVID-19 pandemic, people have been wearing masks for a long period of time during their daily lives, which may have increased exposure to a certain number of phthalates of an average level of 1950 ng/g, determined in mask samples [9].

Epidemiological and toxicological studies have shown that exposure to PAEs through indoor sources may be related to carcinogenesis, the disruption of the endocrine system, and other symptoms [2]. As a kind of endocrine disruption, PAEs have an impact on the endocrine system and the genital system [10]. Animal [11], as well as human [12], sampling tests indicated that PAEs will cause damage to the reproductive system and the testicular function of males. In addition, epidemiology investigations suggested that early puberty

in females is related to DEHP exposure [13,14], which may also raise the risk of breast cancer and endometriosis [15]. Besides the adverse effects on the endocrine system and the reproductive system, PAEs may even cause allergies, asthma [16], and cancer [17,18].

PAEs enter the human body through three kinds of intake ways: inhalation, oral ingestion, and dermal penetration [19]. The mechanism of emission of PAEs from sources and their transport fate indoors have been basically clarified by many studies [20–22] so that the indoor concentration of PAEs can be predicted or estimated with accepted accuracy by the models, together with numerous measured values in different countries and regions [1,23]. At the same time, the indoor concentration of phthalate ester and its metabolism in urine and blood in different countries and regions has also been measured for health risk assessments [24–26]. However, the relationship between indoor exposure to phthalate and metabolisms has been not established, and the prediction of internal exposure based on the external exposure to PAEs is difficult. Recently, some researchers have attempted to explore the issue of how PAEs entered human bodies based on some PBPK (physiologically based pharmacokinetic) models cooperated with intakes of dermal penetration and inhalation, as well as some experimental data [27–29]. However, the detrimental health outcomes of different intake pathways still cannot be compared in the mechanism. In addition, for linking external exposure to DEHP with internal exposure, the distribution of PAEs in the body's organs and tissues after entering the human body through three pathways, including inhalation, oral ingestion, and dermal penetration, still needs to be investigated. What is more, some important organs and tissues are not specified in those models, so the internal exposure to PAEs and their substitutes in these organs and tissues cannot be estimated. Therefore, the objective of this paper is to made a preliminary study on this issue by using a whole-body PBPK model. This PBPK model can simulate targeted organs and tissues through different intake pathways and therefore can be beneficial to study how the accumulation of PAEs leads to detrimental health outcomes in different organs in the human body.

2. Materials and Methods

2.1. Model Description

Generally, physiologically based pharmacokinetic (PBPK) models are used for decisions in drug invention and developments and can simulate simultaneous concentrations of drugs with time in different organs and tissues after a specified dosing. Recently, some studies have employed PBPK models to investigate contaminants' exposure and their metabolism variation with time after exposure [29]. In this paper, we referred to the generic 14-compartments PBPK model in the Simbiology platform in Matlab [30]. As studies have shown that DEHP might have the adverse effects on carcinogenesis, the disruption of the endocrine system, asthma, and other symptoms [16,31], the simulation chose the liver, the lungs, and the endocrine system (the spleen and the pancreas) as target organs to simulate their accumulation time course. The original model assumes that drugs are well stirred and absorption rates are determined merely by transcellular or paracellular permeability and solubility to access the accuracy of the prediction. However, this model cannot be applied well to predict the concentration-time profiles of PAEs in human organs in three different ways (inhalation, oral ingestion, and dermal penetration). So as shown in Figure 1, we divided the original model into numerous compartments: the lungs, the heart, the brain, the muscles, the skin, the liver, the gut, the spleen, the pancreas, the bones, the kidneys, urine, the thymus, arterial blood, venous blood, and the rest of the organs. The blue lines represent the DEHP flow between organs, and the red ones represents the MEHP towards the organs. Among the organs, urine, which represents the excretion of the human body, was regarded as a compartment with a volume of 1 milligram. Additionally, the compartment representing the rest of organs only presented the metabolism and delivery of MEHP as the hydrolysis product of DEHP. DEHP entered the body through the gut, the lungs, and the skin, representing the three pathways of ingestion intake, inhalation, and dermal penetration, respectively.
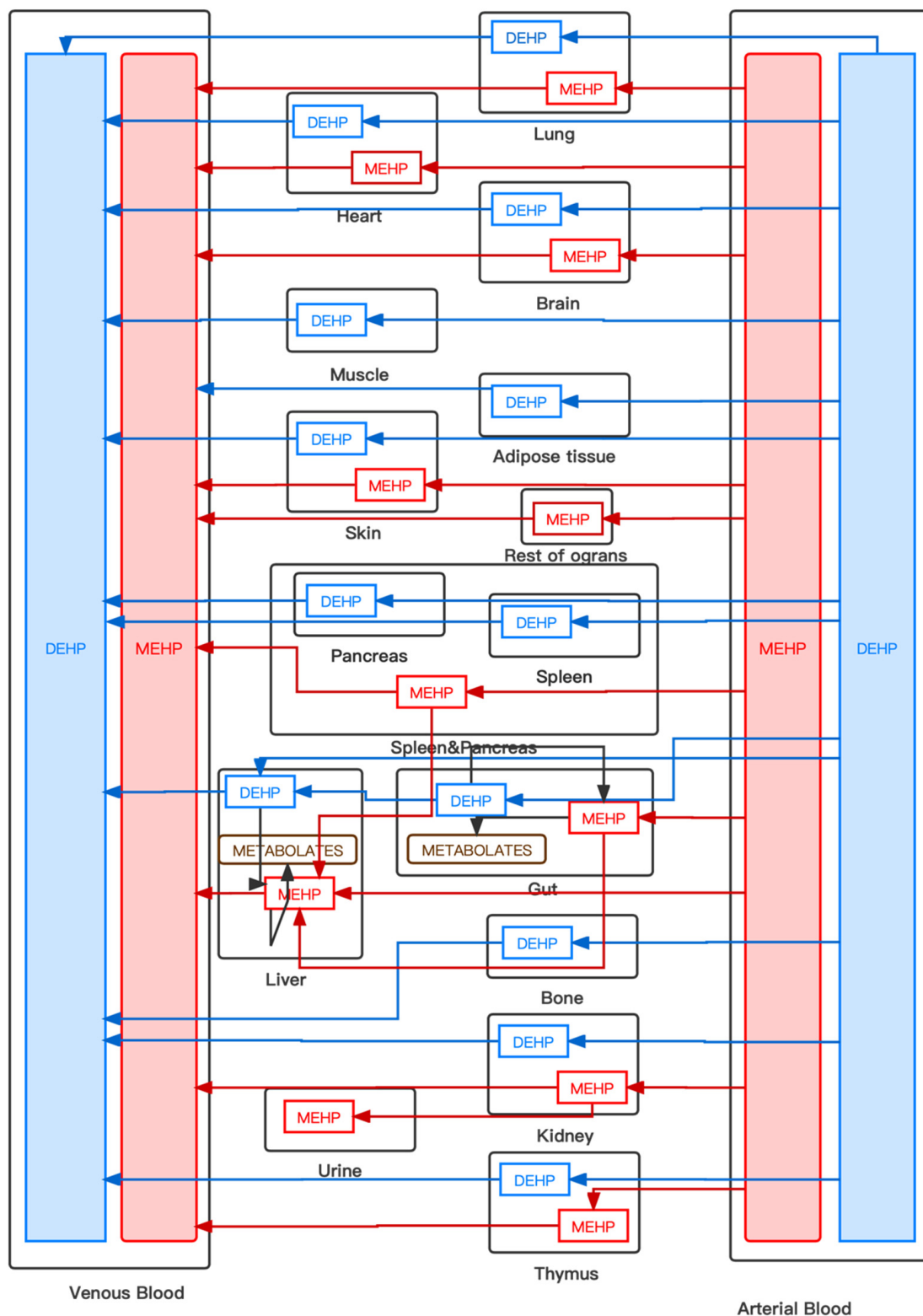
Figure 1. The framework of the PBPK model.

The reactions between the species in the PBPK model were referred to in Sharma's modeling approach's modeling approach [27], which mainly discussed 5 metabolites: MEHP, mono (2-ethyl-5-hydroxyhexyl) phthalate (5-OH MEHP), mono (2-ethyl-5-oxohexyl) phthalate (5oxo-MEHP), mono (2-ethyl-5-carboxypentyl) phthalate (5cx MEPP), and phthalic acid

Int. J. Environ. Res. Public Health **2022**, 19, 5742

4 of 15

esters. It was only kinetic in the intestines and the liver [25], and only MEHP was concerned with simplification. The main governing equations are shown in Supplementary File S1.

2.2. Model Parameter

As shown in Table 1, the parameters of the chemical and physical properties of DEHP and MEHP in the reactions in the PBPK model were referred to in Sharma's modeling approach [27]. The basic human body parameters such as organ capacity in Table 2 refer to the original PBPK model [30]. Due to the lack of a link between the parameters and MEHP delivery, as well as the metabolism in the original model built by Peters, more related parameters were referred to Sharma and applied in the improved model. According to Sharma's research, the model parameters are distributed log normally in the range of ±1 to ±1.5 standard deviations. By estimating uncertainty, the value was picked by selecting a random value first and ran by the Monte Carlo simulations. After 20,000 iterations, the collected output values formed a random sample. However, in this model, the parameters simplify chose the mean value.

Table 1. The PBPK model parameter.

Parameters	Symbol	Unit	Values/ Contribution	Reference
Molecular weight (DEHP)	MW	g/mole	391	-
Molecular weight (D4-MEHP)	MW	g/mole	281	[28]
Molecular weight (MEHP-OH)	MW	g/mole	297	[28]
Molecular weight (D4-5-oxo MEHP)	MW	g/mole	295	[28]
Molecular weight (D4-5-cx MEPP)	MW	g/mole	311	[28]
Octanol: water partition coefficient	LogKo:w	N	7.6	-
Partition coefficients				
Gut/plasma	k_gut_plasma	N	LN [a] (12.86,1.1)	-
Liver/plasma	k_liver_plasma	N	LN [a] (10.16,1.1)	-
Fat/plasma	k_fat_plasma	N	LN [a] (188, 1.1)	-
Rest of the body/plasma	k_restbody_plasma	N	LN [a] (6.24, 1.1)	-
Liver/plasma	k_liver_plasmaM1	N	LN [a] (1.7, 1.1)	[32]
Fat/plasma	k_fat_plasmaM1	N	LN [a] (0.12, 1.1)	[32]
Rest of the body/plasma	k_restbody_plasmaM1	N	LN [a] (0.38, 1.1)	[33]
Uptake rate of 5-OHMEHP to blood	KtM2	1/h	LN [a] (0.07, 1.5)	[34]
Uptake rate of 5-oxo MEHP to blood	KtM4 cytosol maximum reaction value	1/h	LN [a] (0.08, 1.5)	[34]
Absorption and elimination parameters				
Unbound fraction in plasma for MEHP	fup	N	0.007	[35]
Oral absorption rate	kgut	1/h	LN [a] (7, 1.5)	[35]
Elimination constant	kurine	1/h	LN [a] (0.35, 1.1)	[27]
Metabolic parameters for DEHP and its metabolites in the intestines and the liver				
DEHP to MEHP in intestinal MSP [b] maximum reaction value	vmaxgutM1	μg/min/mg MSP [b]	LN [a] (0.11,1.1) [c]	[36]
DEHP to MEHP in gut cytosol MSP [b] maximum reaction value	vmaxgut_cytM1	μg/min/mg	LN [a] (0.312,1.1) [c]	[36]
MEHP to 5-OH MEHP maximum reaction value	vmaxgutM2	μg/min/mg MSP [b]	LN [a] (0.0012,1.1) [c]	[36]
MEHP to 5-carboxy MEPP maximum reaction value	vmaxgutM3	μg/min/mg MSP [b]	0	[36]
MEHP-OH to 5-oxo MEHP maximum reaction value	vmaxgutM4	μg/min/mg MSP [b]	LN [a] (0.0012,1.5) [c]	[36]
MEHP to phthalic acid esters maximum reaction value	vmaxgutM5	mg/min/mg MSP [b]	LN [a] (0.285, 1.1) [c]	[36]

Int. J. Environ. Res. Public Health **2022**, *19*, 5742

5 of 15

Table 1. *Cont.*

Parameters	Symbol	Unit	Values/ Contribution	Reference
Metabolic parameters for DEHP and its metabolites in the intestines and the liver				
Conc. at half maximum value	kmgutM1	µg/L	6956	[36]
Conc. at half maximum value	kmgutM2	µg/L	22508	[36]
Conc. at half maximum value	kmgutM3	µg/L	0	[36]
Conc. at half maximum value	kmgutM4	µg/L	219076	[36]
Conc. at half maximum value	kmgutM5	µg/L	187652	[36]
Conc. at half maximum value	kmgut_cytM1	µg/L	7038	[36]
DEHP to MEHP in liver MSP maximum reaction value	vmaxliverM1	µg/min/mg MSP [b]	LN [a] (0.112, 1.1) [c]	[36]
DEHP to MEHP in liver cytosol maximum reaction value	vmaxliverM1_cyt	µg/min/mg	LN [a] (0.036, 1.1) [c]	[36]
MEHP to 5-OH MEHP maximum reaction value	vmaxliverM2	µg/min/mg MSP [b]	LN [a] (0.172, 1.1) [c]	[36]
MEHP to 5-carboxy MEPP maximum reaction value	vmaxlivM3	µg/min/mg MSP [b]	LN [a] (0.0023, 1.5) [c]	[36]
MEHP-OH to 5-oxo MEHP maximum reaction value	vmaxlivM4	µg/min/mg MSP [b]	LN [a] (0.003, 1.1) [c]	[36]
MEHP to phthalic acid esters maximum reaction value	vmaxlivM5	µg/min/mg MSP [b]	LN [a] (0.088, 1.1) [c]	[36]
Conc. at half maximum value	kmliver_cytM1	µg/L	2228.7	[36]
Conc. at half maximum value	kmliverM2	µg/L	7980.4	[36]
Conc. at half maximum value	kmliverM3	µg/L	1124	[36]
Conc. at half maximum value	kmliverM4	µg/L	23117.7	[36]
Conc. at half maximum value	kmliverM5	µg/L	141315	[36]

[a] LN represents that the model parameters are distributed log normally in the range of ±1 to ±1.5 standard deviations. [b] MSP represents the macrophage stimulating protein. [c] The parameter value needs to be scaled to the whole body weight prior to the model.

Table 2. The organs' capacity [30].

Compartment	Unit	Value
Arterial Blood	milliliter	1698
Bone	milliliter	4579
Brain	milliliter	1450
Gut	milliliter	1650
Heart	milliliter	310
Kidney	milliliter	280
Liver	milliliter	1690
Lungs	milliliter	1172
Muscle	milliliter	35,000
Pancreas	milliliter	77
Rest other organs	milliliter	49,579
Skin	milliliter	7800
Spleen	milliliter	192
Thymus	milliliter	29
Urine	milliliter	1
Venous Blood	milliliter	3396

2.3. Dose in PBPK Model

In this paper, DEHP was chosen as the target compound due to its ubiquitous existence in indoor environments. Three different dosing scenarios, as shown in Figure 2, were adopted to represent the process of DEHP entering the human body through inhalation, oral ingestion, and dermal penetration. For dermal penetration, pertinent studies showed that for those small-molecular-weight PAEs, dermal penetration contributes to a dominant intake compared to inhalation [37,38]. Additionally, a later study also proved that,

Int. J. Environ. Res. Public Health **2022**, 19, 5742

6 of 15

compared to inhalation, skin exposure has a greater impact on the human body through a more detailed model and experimental studies [19,39]. For inhalation, due to the filtration of nasal mucosa, some of the chemical compounds can be effectively blocked. For oral ingestion, the model assumed that the intake amount of DEHP is correlated to the intake amount of food.
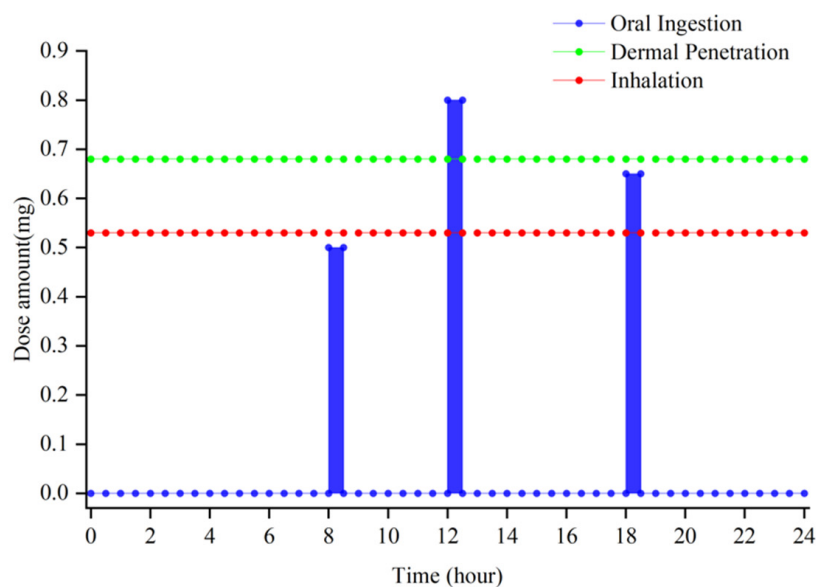

Figure 2. The amount of the three-dose set in the PBPK model.

Based on the studies above and a field investigation of health exposure to DEHP, we set a new dosing amount of three kinds of intake.

According to the estimated data from studies [40,41], dermal penetration and inhalation were both set as continuous doses with amounts of 0.68 mg/h and 0.53 mg/h, respectively, because the human body was assumed to be exposed to an indoor contaminated environment all day. According to the research [42], the mean dietary intake of DEHP in the general population was 2.34 µg/kg/day, and 97.5% of the intake in the general population was 5.22 µg/kg/day. Therefore, the total intake amount of oral ingestion was set as 1.95 mg (3.25 µg/kg/day, 60 kg). The oral ingestion was assumed as 3 times with dinners at 8:00 am, 12:00 pm, and 18:00 pm, respectively, in one day (the duration of one intake lasts for 30 min). Meanwhile, based on the average amount of food intake of a person, the ratio for breakfast, lunch, and supper is 0.5:0.8:0.65 with regard to the different amounts of food. Other oral ingestion was neglected for the purposes of simplification.

3. Results and Discussion

3.1. Validation of PBPK Model

The validation of the new PBPK model was tested by the experimental data of metabolites of DEHP in the human urine and serum after single oral doses of deuterium-labelled DEHP [36]. According to Koch, the single dose was 48.1 mg (0.65 mg/kg body-weight, a male volunteer weighting 75 kg). We set the oral dose of the same amount in the PBPK model, and the time profile of the absolute accumulative excretion of MEHP in urine was shown in Figure 3. According to the figure, the MEHP accumulation (mg) in the urine of the simulation and of the experiment ascended with a similar trend and gradually reached an equilibrium at the amounts of 3.000 mg and 2.475 mg, respectively. Figure 4 shows that the trend and the peak of the MEHP concentration in the plasma between the simulation of the model and of the reference coincided, which suggests that the result validated the rationality of the model. According to figures, the MEHP amount of the excretion, as well as the concentration in plasma of the simulation, were comparatively higher than those of the experiment. This may indicate that the simulated human body in the model has greater

Int. J. Environ. Res. Public Health **2022**, *19*, 5742

7 of 15

metabolic capacity than the volunteer in Koch experiment. Another potential reason for the bias is the uncertainty of the estimated parameters in the model. This needs to be studied further in the future to estimate the parameters more accurately.
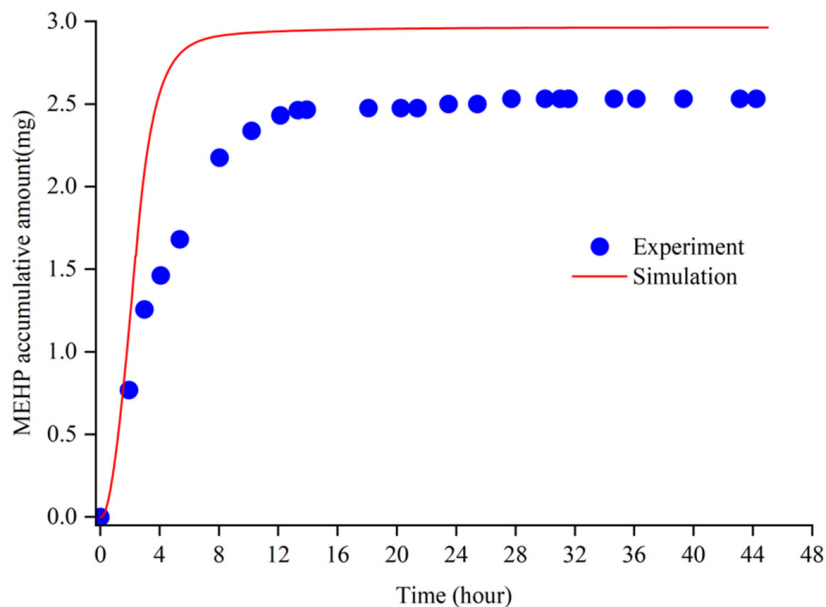

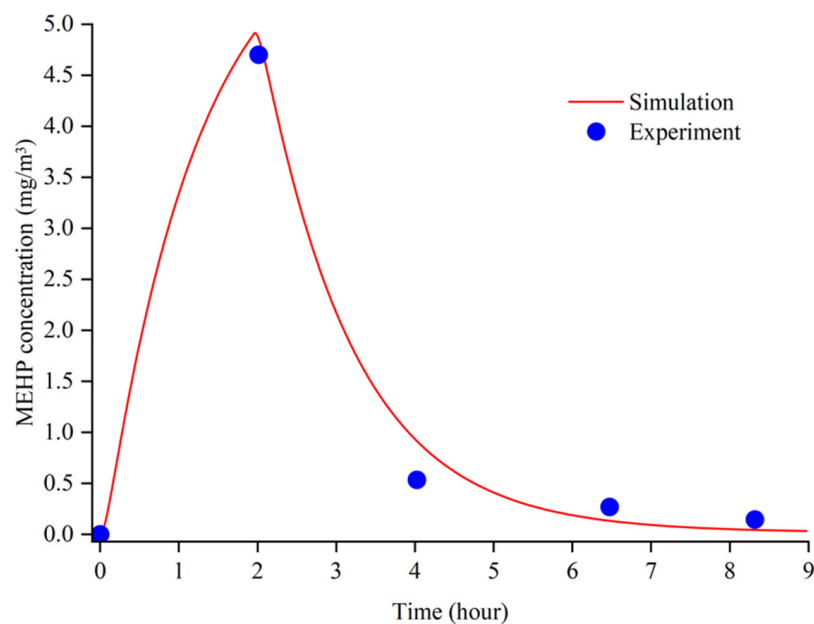**Figure 3.** The MEHP accumulative excretion in the urine between the experiment and the simulation.

Figure 4. The MEHP concentration in the plasma between the experiment and the simulation.

3.2. DEHP and MEHP Concentration in Different Organs and Tissues through Three Sifferent Intake Pathways

According to Figure 5, a 24-h dose could not be metabolized and excreted adequately until 48 h. This finding suggests that the leftover of DEHP the day before would affect the DEHP accumulative concentration the next day, which, on the other hand, could be out of consideration at the third day. Shown in Table 3, the error between 24 h and 48 h was in the range of 1.7924% to 2.004%, which cannot be ignored, while the difference between 48 h and 72 h was 0.0979% to 0.0674%, and the following error was getting smaller gradually. Regarding the human intakes of different kinds of PAEs in their daily lives, to study the

actual effect of accumulative DEHP and MEHP in the human body, simulation is needed for at least 48 h.
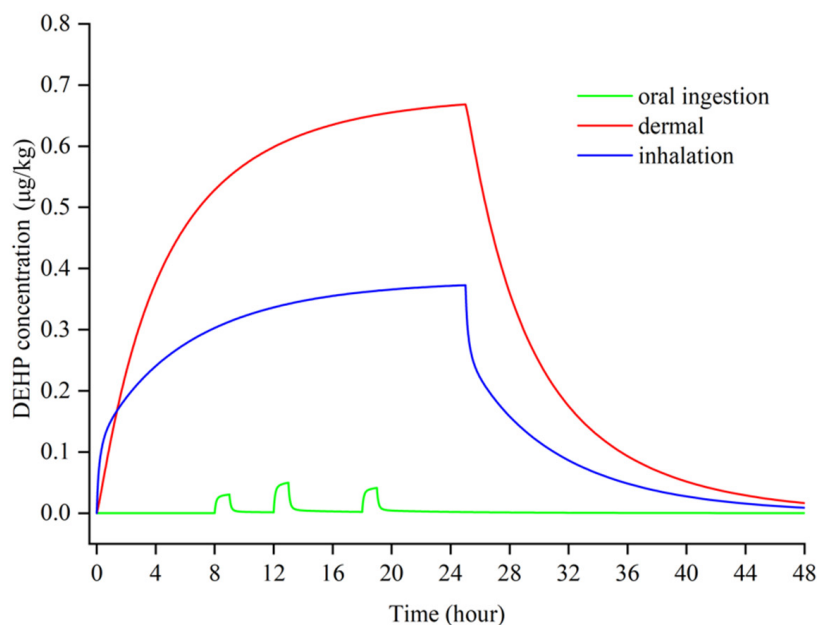

Figure 5. The total accumulation through three intake methods under 24 h doses.

Table 3. The difference between each day.

	δ (24 h–48h) (%)	δ (48 h–72 h) (%)	δ (72 h–96 h) (%)	δ (96 h–120 h) (%)
Oral ingestion	2.0044	0.0674	0.0023	0.0001
Inhalation	2.0869	0.0700	0.0024	0.0001
Dermal penetration	1.7294	0.0979	0.0032	0.0002

3.2.1. Oral Ingestion

Figure 6 shows that DEHP quickly accumulated in the organs after entering the human body through scheduled oral doses (0.5 mg at 8 h, 0.8 mg at 12 h, 0.65 mg at 18 h, 0.5 mg at 32 h, 0.8 mg at 36 h, and 0.65 mg at 42 h). Among the organs, the DEHP concentration accumulated most in the liver and reached a maximum value (2.608×10^{-3} μg/mL at 33 h, 4.180×10^{-3} μg/mL at 37 h, and 3.404×10^{-3} μg/mL at 43 h) within an hour after the intakes (at this time, each organ rapidly reached the cumulative peak). The highest DEHP concentration in the lungs, the spleen, and the pancreas (ranging from 9.221×10^{-4} μg/mL to 9.677×10^{-4} μg/mL at 33h, 1.512×10^{-3} μg/mL to 1.584×10^{-3} μg/mL at 37 h, and 1.275×10^{-3} μg/mL to 1.333×10^{-3} μg/mL at 43 h, respectively) was basically a half lower than the DEHP concentration in the liver, indicating that the intake of oral ingestion has the greatest adverse effect on liver. After reaching the peak, the DEHP in various organs quickly metabolized. As shown in the figure, the concentration of DEHP dramatically reduced in a short period of time. As the scheduled oral doses are constantly absorbed, the fewest cumulative concentration of DEHP in human body still remained in the range of 10^{-5} μg/mL to 10^{-6} μg/mL.

Figure 7 indicates the change of MEHP concentration in the organs though oral ingestion. Compared to the organs of the DEHP concentration simulation, the spleen and pancreas combined to form a whole endocrine system. As the hydrolysis product of DEHP, MEHP is gradually generated during the hydrolysis and metabolites at the same time, causing a trend of a constant increase in the first hour and then a reduction at a steady rate. According to Figure 7 compared to the time course of DEHP concentration, the curves of MEHP concentration in different organs showed the same order of the

accumulative amount. The greatest distribution of the MEHP concentration was still in the liver (2.862×10^{-3} µg/mL at 33 h, 4.669×10^{-3} µg/mL at 37 h, and 3.759×10^{-3} µg/mL at 43 h, respectively), which was nearly two times as many as the accumulation zenith in the lungs and the endocrine system.
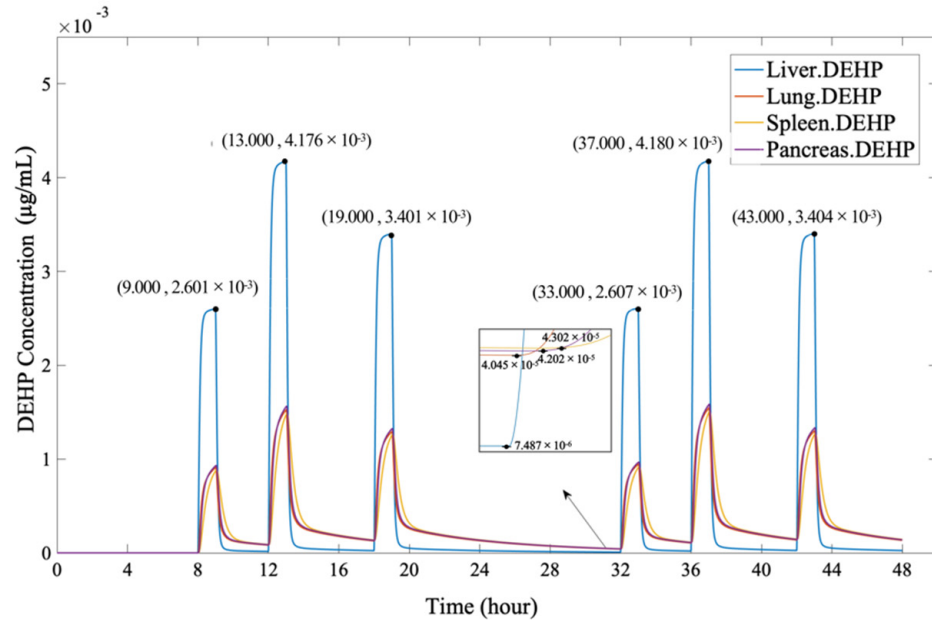

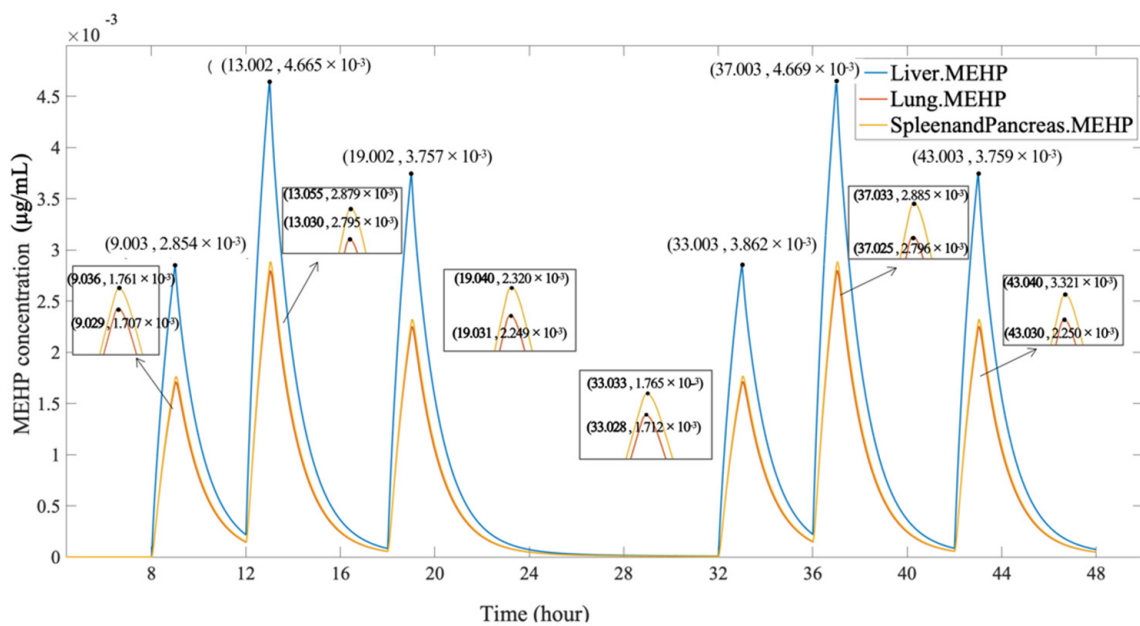**Figure 6.** The DEHP concentration in organs, through oral ingestion.

Figure 7. The MEHP concentration in the organs, through oral ingestion.

3.2.2. Dermal Penetration

In the model, the dose through dermal penetration was continuously supplied. As a result, the DEHP concentration through skin rises gradually at first and then reaches equilibrium at a later stage. As the penetration through skin was a continuous dose, the accumulative concentration of DEHP through dermal penetration was, on average, an order of magnitude higher than the oral ingestion.

Figure 8 shows that the DEHP concentration among organs though dermal penetration increased at a steady rate until it reached a peak within 30 h and then reached an equilibrium

concentration. The greatest equilibrium accumulation through dermal penetration was in the spleen and the pancreas (4.131×10^{-2} µg/mL). However, the DEHP concentration in the liver was the lowest among the organs (7.316×10^{-3} µg/mL), indicating that the dose through the skin may have had less of an impact on liver. What is more, the equilibrium concentration of the lungs (4.004×10^{-2} µg/mL) was slightly lower than that in the spleen and the pancreas.
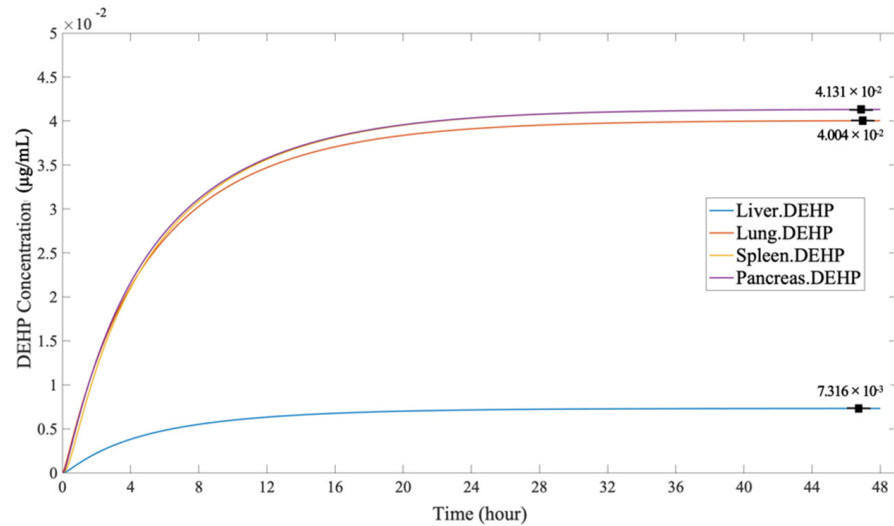

Figure 8. The DEHP concentration in the organs, through dermal penetration.

Figure 9 shows the time-concentration profile of MEHP in various organs through dermal penetration. Compared to the curves of DEHP concentration in different organs, the time profile of MEHP showed a different order of the accumulative number of organs. The MEHP concentration in the liver (6.798×10^{-3} µg/mL) was markedly higher than the concentration in the endocrine system (4.383×10^{-3} µg/mL) and the lungs (4.248×10^{-3} µg/mL). This phenomenon can be explained by the fact that the DEHP in the liver was mostly metabolized and decomposed to MEHP and its other hydrolysates. In the MEHP simulation, the concentration of liver was still the greatest; however, the accumulation in the lungs and the endocrine system cannot be ignored. This simulation further proves that phthalates exposure has great potential adverse detrimental health outcomes on the liver.
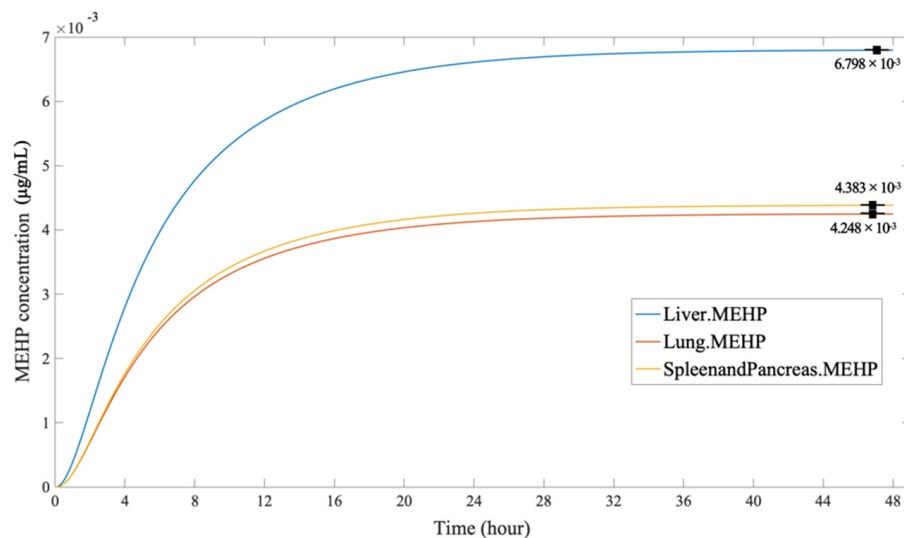

Figure 9. The MEHP concentration in the organs, through dermal penetration.

3.2.3. Inhalation

As a continuous dose, the method of inhalation distributes the lower intake amount of DEHP than the dermal penetration. The trend of DEHP concentration was similar to the dermal penetration but reached an equilibrium more rapidly, suggesting that DEHP in the lungs might transfer and decompose faster. According to the Figure 10 the descending order of the equilibrium peak of DEHP was the spleen and pancreas (3.221×10^{-2} µg/mL), the lungs (3.122×10^{-3} µg/mL), and the liver (5.703×10^{-3} µg/mL).
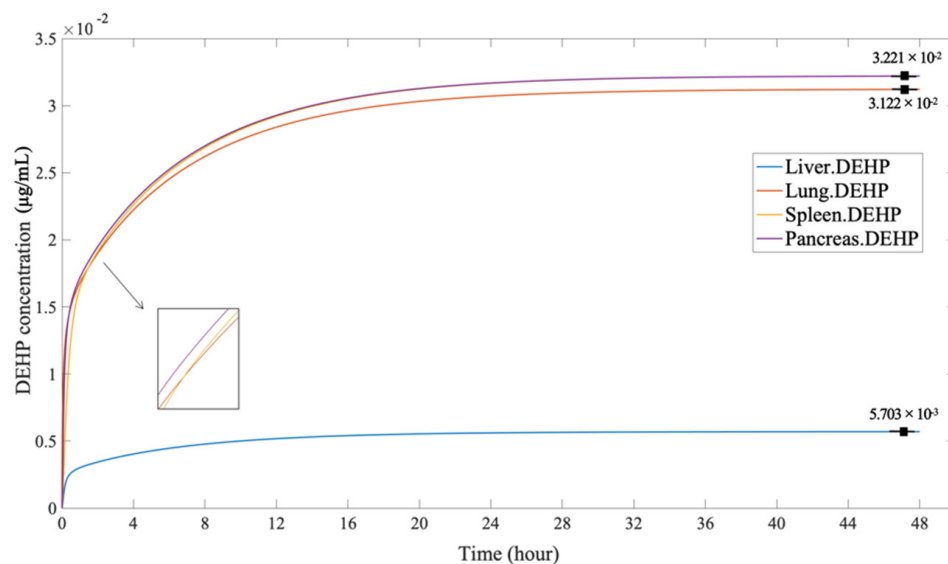

Figure 10. The DEHP concentration in the organs, through inhalation.

According to Figure 11 the MEHP concentration through inhalation shared a similar rising trend but a disparity in the order of the equilibrium amount in the organs. Among the organs, the liver still had the highest MEHP equilibrium concentration (5.299×10^{-3} µg/mL). However, the difference between the lungs ($3,311 \times 10^{-3}$ µg/mL) and the endocrine system (3.416×10^{-3} µg/mL) was small. As the liver and the gut are the only organs that can metabolize in the PBPK model, this result further proved that the DEHP in the liver was mostly metabolized and hydrolyzed to MEHP and other small molecule compounds.
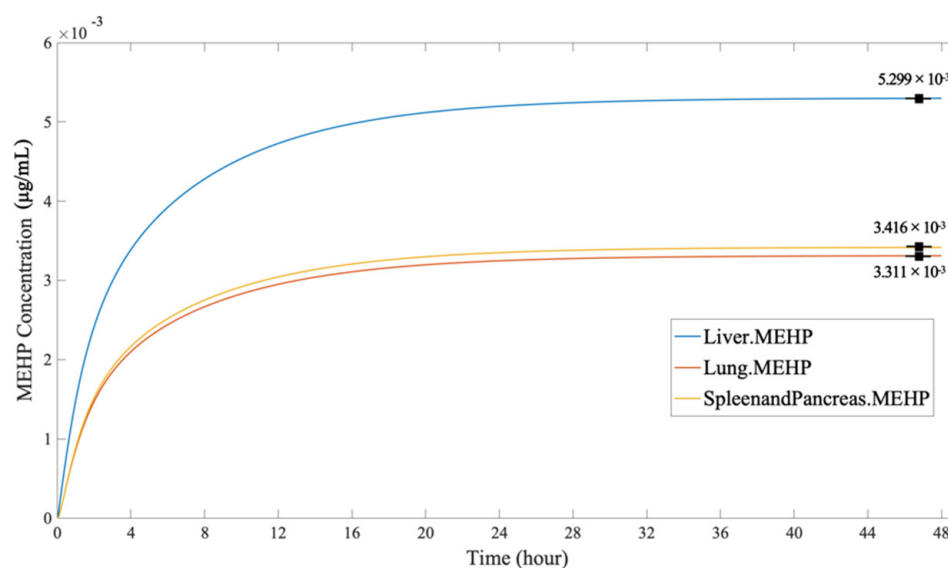

Figure 11. The MEHP concentration in the organs, through inhalation.

3.3. Further Comparison and Health Care Assessment through Three Different Doses

The simulation showed that the constant and scheduled intake of phthalates cannot be metabolized and excreted entirely. The majority of DEHP can be metabolized in the first 48 h after intake. Few compounds (DEHP and its metabolites) remain in the body, and those parts of the compounds will eventually lead to potential detrimental health outcomes. This simulation result can be proved by Anderson et al., who suggest that the metabolites of DEHP excreted 47.1 ± 8.5% on a molar basis within 48 h [33]. Through the simulation, the intake of dermal penetration, as a repeated dose with a greater amount, distributes the greatest accumulation in most of the organs, while the oral ingestion, ignoring the breathing behavior via mouth, only intakes DEHP through dinners and therefore accumulates medially an order of magnitude lower than other two doses.

Studies have proved that DEHP and its hydrolysis product, MEHP, can do damage to human organs. According to Figures 12 and 13, among all the selected organs, the lung, the pancreas, and the spleen accumulate more DEHP, while the liver accumulates smaller molecule compounds, MEHP. This result shows the metabolic function of the liver and further suggests the non-negligible accumulation of PAEs in different organs. The link with actual pathological studies, and phthalates accumulation in the liver, might have an impact on the pathways of some essential receptors in the liver that control not only xenobiotic detoxification but also energy homeostasis and the circadian clock [43]. The excessive accumulation of DEHP in liver might inhibit liver detoxifying enzymes and result in liver dysfunction [44].
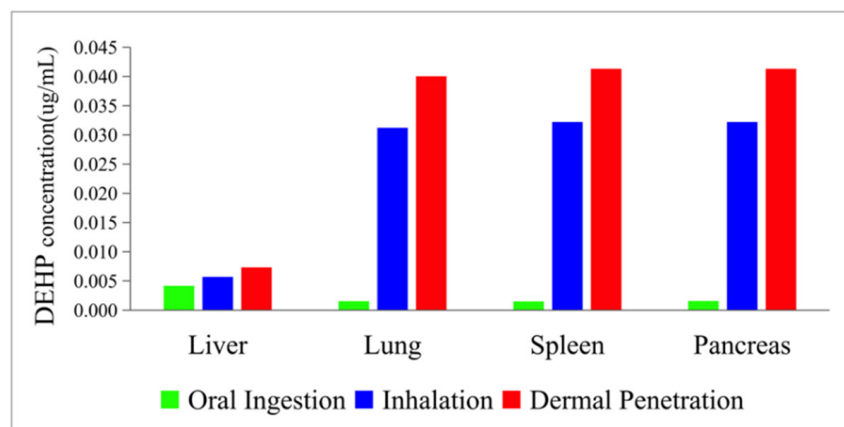

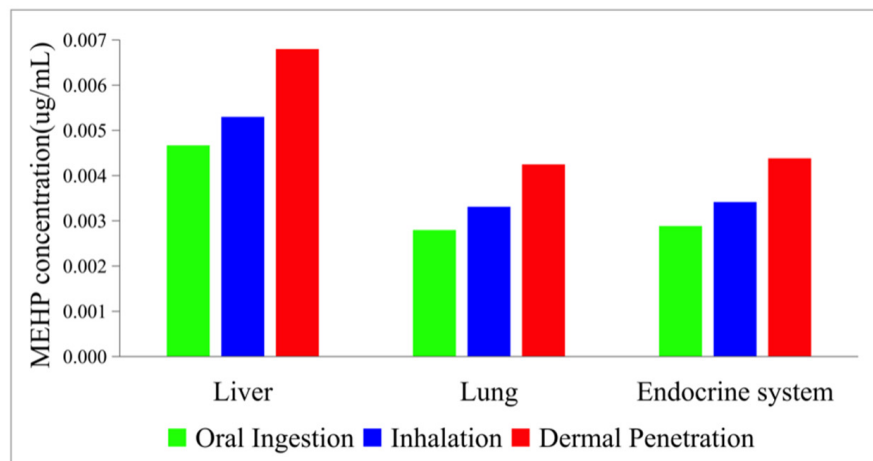**Figure 12.** The maximum DEHP concentration in the organs.

Figure 13. The maximum MEHP concentration in the organs.

What is more, DEHP might cause significant decreases in cell viability and impaired antioxidant systems [45], which might cause endocrine system disorders. Research also showed that particularly low molecular weight phthalates were associated with poorer lung function [46]. After all, the simulation suggests that the DEHP might have toxicity to human lung epithelial A549 cells and eventually cause DNA damage, oxidative stress, apoptosis, and estrogenic effects [47].

4. Conclusions

From the results, the proposed whole-body PBPK model is able to predict the internal exposure of DEHP and its metabolites through three pathways into the body: inhalation, oral ingestion, and dermal penetration. Through the simulation, among three doses, the intake of dermal penetration distributes the greatest accumulation in most of the organs, indicating that the intake through the skin may be the main intake method of daily exposure. The intake of dermal penetration and inhalation, as a continuous dose, leads to the equilibrium concentration of DEHP and MEHP in different organs and tissues (ranging from 10^{-2} to 10^{-3} µg/mL). While oral ingestion, distributing the lowest accumulation through the three kinds of intake pathways, retains much less concentration at the end of every day (ranging from 10^{-5} to 10^{-6} µg/mL). Additionally, the simulation result demonstrates that the endocrine system and the lung accumulate more DEHP, but the liver, as the main metabolizing organ, accumulate more small molecule compounds, MEHP. Certainly, the model still has potential. The simulation result that the DEHP concentration in the lungs through inhalation was less than the dermal penetration still needs to be discussed. We suggest that the amount of DEHP will decrease through transportation due to the adhesion or other mechanisms. However, the model assumes arterial blood and venous blood as a single compartment, respectively. This flaw lacks detailed reactions to account for the inevitable loss while the drug is flowing through vessels. What is more, as the physical and chemical properties of the chemical compounds can be adjusted, the PBPK model was believed to be compatible with other kinds of doses. To encourage reactions of various molecule compounds, the model can also be simulated with a greater framework of detailed profiles in the human body. This PBPK model can be beneficial if linked with pathology and environmental science.

Supplementary Materials: The following supporting information can be downloaded at: https: //www.mdpi.com/article/10.3390/ijerph19095742/s1, File S1: Supporting Materials: Standard ordinary differential equations used in tissue dosimetry model.

Author Contributions: Conceptualization, X.W., A.L. and K.L.; methodology, X.W. and A.L.; software, X.W.; validation, A.L., L.K. and K.L.; formal analysis, R.L.; investigation, A.L.; resources, S.W.; data curation, A.L. and L.K.; writing—original draft preparation, A.L.; writing—review and editing, X.W.; visualization, L.K.; supervision, X.W.; project administration, X.W.; and funding acquisition, X.W. All authors have read and agreed to the published version of the manuscript.

Institutional Review Board Statement: Not applicable.

Informed Consent Statement: Not applicable.

Data Availability Statement: Adapted with permission from ref. [30]. 2008 Peters, S.A.

Conflicts of Interest: The authors declare no conflict of interest.

References

1. Wang, X.; Tao, W.; Xu, Y.; Feng, J.; Wang, F. Indoor phthalate concentration and exposure in residential and office buildings in Xi'an, China. *Atmos. Environ.* **2014**, *87*, 146–152. [CrossRef]
2. Chang, W.-H.; Herianto, S.; Lee, C.-C.; Hung, H.; Chen, H.-L. The effects of phthalate ester exposure on human health: A review. *Sci. Total Environ.* **2021**, *786*, 147371. [CrossRef] [PubMed]

3. Preece, A.-S.; Shu, H.; Knutz, M.; Krais, A.M.; Wikström, S.; Bornehag, C.-G. Phthalate levels in indoor dust and associations to croup in the SELMA study. *J. Expo. Sci. Environ. Epidemiol.* **2021**, *31*, 257–265. [CrossRef] [PubMed]

4. Huang, C.; Zhang, Y.-J.; Liu, L.-Y.; Wang, F.; Guo, Y. Exposure to phthalates and correlations with phthalates in dust and air in South China homes. *Sci. Total Environ.* **2021**, *782*, 146806. [CrossRef] [PubMed]

5. Dobaradaran, S.; Akhbarizadeh, R.; Mohammadi, M.J.; Izadi, A.; Keshtkar, M.; Tangestani, M.; Moazzen, M.; Shariatifar, N.; Mahmoodi, M. Determination of phthalates in bottled milk by a modified nano adsorbent: Presence, effects of fat and storage time, and implications for human health. *Microchem. J.* **2020**, *159*, 105516. [CrossRef]

6. Mehraie, A.; Shariatifar, N.; Arabameri, M.; Moazzen, M.; Mortazavian, A.M.; Sheikh, F.; Sohrabvandi, S. Determination of phthalate acid esters (PAEs) in bottled water distributed in tehran: A health risk assessment study. *Int. J. Environ. Anal. Chem.* **2022**, *102*, 1–15. [CrossRef]

7. Zhang, Y.; Lin, L.; Cao, Y.; Chen, B.; Zheng, L.; Ge, R.-S. Phthalate Levels and Low Birth Weight: A Nested Case-Control Study of Chinese Newborns. *J. Pediatr.* **2009**, *155*, 500–504. [CrossRef]

8. Zhang, J.; Sun, C.; Lu, R.; Zou, Z.; Liu, W.; Huang, C. Associations between phthalic acid esters in household dust and childhood asthma in Shanghai, China. *Environ. Res.* **2021**, *200*, 111760. [CrossRef]

9. Xie, H.; Han, W.; Xie, Q.; Xu, T.; Zhu, M.; Chen, J. Face mask—A potential source of phthalate exposure for human. *J. Hazard. Mater.* **2021**, *422*, 126848. [CrossRef]

10. Høyer, B.B.; Lenters, V.; Giwercman, A.; Jönsson, B.A.G.; Toft, G.; Hougaard, K.S.; Bonde, J.P.E.; Specht, I.O. Impact of Di-2-Ethylhexyl Phthalate Metabolites on Male Reproductive Function: A Systematic Review of Human Evidence. *Curr. Environ. Health Rep.* **2018**, *5*, 20–33. [CrossRef]

11. Lea, R.G.; Byers, A.S.; Sumner, R.N.; Rhind, S.M.; Zhang, Z.; Freeman, S.L.; Moxon, R.; Richardson, H.M.; Green, M.; Craigon, J.; et al. Environmental chemicals impact dog semen quality in vitro and may be associated with a temporal decline in sperm motility and increased cryptorchidism. *Sci. Rep.* **2016**, *6*, 31281. [CrossRef] [PubMed]

12. Chang, W.-H.; Wu, M.-H.; Pan, H.-A.; Guo, P.-L.; Lee, C.-C. Semen quality and insulin-like factor 3, Associations with urinary and seminal levels of phthalate metabolites in adult males. *Chemosphere* **2017**, *173*, 594–602. [CrossRef] [PubMed]

13. Watkins, D.J.; Sánchez, B.N.; Téllez-Rojo, M.M.; Lee, J.M.; Mercado-García, A.; Blank-Goldenberg, C.; Peterson, K.E.; Meeker, J.D. Faculty Opinions recommendation of Phthalate and bisphenol A exposure during in utero windows of susceptibility in relation to reproductive hormones and pubertal development in girls. *Environ. Res.* **2017**, *159*, 143–151. [CrossRef] [PubMed]

14. Hashemipour, M.; Kelishadi, R.; Amin, M.M.; Ebrahim, K. Is there any association between phthalate exposure and precocious puberty in girls? *Environ. Sci. Pollut. Res.* **2018**, *25*, 13589–13596. [CrossRef]

15. Mughees, M.; Chugh, H.; Wajid, S. Mechanism of phthalate esters in the progression and development of breast cancer. *Drug Chem. Toxicol.* **2020**, *45*, 1021–1025. [CrossRef]

16. Bornehag, C.-G.; Sundell, J.; Weschler, C.J.; Sigsgaard, T.; Lundgren, B.; Hasselgren, M.; Hägerhed-Engman, L. The Association between Asthma and Allergic Symptoms in Children and Phthalates in House Dust: A Nested Case–Control Study. *Environ. Health Perspect.* **2004**, *112*, 1393–1397. [CrossRef]

17. Chuang, S.-C.; Chen, H.-C.; Sun, C.-W.; Chen, Y.-A.; Wang, Y.-H.; Chiang, C.-J.; Chen, C.C.; Wang, S.L.; Chen, C.J.; Hsiung, C.A. Phthalate exposure and prostate cancer in a population-based nested case-control study. *Environ. Res.* **2020**, *181*, 108902. [CrossRef]

18. Warren, J.R.; Lalwani, N.D.; Reddy, J.K. Phthalate esters as peroxisome proliferator carcinogens. *Environ. Health Perspect.* **1982**, *45*, 35–40. [CrossRef]

19. Weschler, C.J.; Bekö, G.; Koch, H.M.; Salthammer, T.; Schripp, T.; Toftum, J.; Clausen, G. Transdermal Uptake of Diethyl Phthalate and Di(*n*-butyl) Phthalate Directly from Air: Experimental Verification. *Environ. Health Perspect.* **2015**, *123*, 928–934. [CrossRef]

20. Xu, Y.; Cohen Hubal, E.A.; Clausen, P.A.; Little, J.C. Predicting Residential Exposure to Phthalate Plasticizer Emitted from Vinyl Flooring: A Mechanistic Analysis. *Environ. Sci. Technol.* **2009**, *43*, 2374–2380. [CrossRef]

21. Liang, Y.; Bi, C.; Wang, X.; Xu, Y. A general mechanistic model for predicting the fate and transport of phthalates in indoor environments. *Indoor Air* **2018**, *29*, 55–69. [CrossRef] [PubMed]

22. Zhou, X.; Lian, J.; Cheng, Y.; Wang, X. The gas/particle partitioning behavior of phthalate esters in indoor environment: Effects of temperature and humidity. *Environ. Res.* **2021**, *194*, 110681. [CrossRef] [PubMed]

23. Karim, A.V.; Krishnan, S.; Sethulekshmi, S.; Shriwastav, A. Phthalate Esters in the Environment: An Overview on the Occurrence, Toxicity, Detection, and Treatment Options. In *New Trends in Emerging Environmental Contaminants*; Singh, S.P., Agarwal, A.K., Gupta, T., Maliyekkal, S.M., Eds.; Springer: Singapore, 2022; pp. 131–160.

24. Huang, S.; Qi, Z.; Ma, S.; Li, G.; Long, C.; Yu, Y. A critical review on human internal exposure of phthalate metabolites and the associated health risks. *Environ. Pollut.* **2021**, *279*, 116941. [CrossRef] [PubMed]

25. Li, Z.; Wu, D.; Guo, Y.; Mao, W.; Zhao, N.; Zhao, M.; Jin, H. Phthalate metabolites in paired human serum and whole blood. *Sci. Total Environ.* **2022**, *824*, 153792. [CrossRef] [PubMed]

26. Choi, G.; Keil, A.P.; Villanger, G.D.; Richardson, D.B.; Daniels, J.L.; Hoffman, K.; Sakhi, A.K.; Thomsen, C.; Herring, A.H.; Drover, S.S.; et al. Pregnancy exposure to common-detect organophosphate esters and phthalates and maternal thyroid function. *Sci. Total Environ.* **2021**, *782*, 146709. [CrossRef] [PubMed]

27. Sharma, R.P.; Schuhmacher, M.; Kumar, V. Development of a human physiologically based pharmacokinetic (PBPK) model for phthalate (DEHP) and its metabolites: A bottom up modeling approach. *Toxicol. Lett.* **2018**, *296*, 152–162. [CrossRef] [PubMed]

28. Wu, Y.; Song, Z.; Little, J.C.; Zhong, M.; Li, H.; Xu, Y. An integrated exposure and pharmacokinetic modeling framework for assessing population-scale risks of phthalates and their substitutes. *Environ. Int.* **2021**, *156*, 106748. [CrossRef]

29. Lorber, M.; Weschler, C.J.; Morrison, G.; Bekö, G.; Gong, M.; Koch, H.M.; Salthammer, T.; Schripp, T.; Toftum, J.; Clausen, G. Linking a dermal permeation and an inhalation model to a simple pharmacokinetic model to study airborne exposure to di(n-butyl) phthalate. *J. Expo. Sci. Environ. Epidemiol.* **2016**, *27*, 601–609. [CrossRef]

30. Peters, S.A. Evaluation of a Generic Physiologically Based Pharmacokinetic Model for Lineshape Analysis. *Clin. Pharmacokinet.* **2008**, *47*, 261–275. [CrossRef]

31. Bornehag, C.G.; Nanberg, E. Phthalate exposure and asthma in children. *Int. J. Androl.* **2010**, *33*, 333–345. [CrossRef]

32. Ziegler, C.G.; Allon, S.J.; Nyquist, S.K.; Mbano, I.M.; Miao, V.N.; Tzouanas, C.N.; Cao, Y.; Yousif, A.S.; Bals, J.; Hauser, B.M.; et al. SARS-CoV-2 Receptor ACE2 Is an Interferon-Stimulated Gene in Human Airway Epithelial Cells and Is Detected in Specific Cell Subsets across Tissues. *Cell* **2020**, *181*, 1016–1035.e9.

33. Anderson, W.A.C.; Castle, L.; Hird, S.; Jeffery, J.; Scotter, M.J. A twenty-volunteer study using deuterium labelling to determine the kinetics and fractional excretion of primary and secondary urinary metabolites of di-2-ethylhexylphthalate and di-iso-nonylphthalate. *Food Chem. Toxicol.* **2011**, *49*, 2022–2029. [CrossRef] [PubMed]

34. Keys, D.A.; Wallace, D.G.; Kepler, T.B.; Conolly, R.B. Quantitative evaluation of alternative mechanisms of blood disposition of di(n-butyl) phthalate and mono(n-butyl) phthalate in rats. *Toxicol. Sci.* **2000**, *53*, 173–184. [CrossRef]

35. Keys, D.A.; Wallace, D.G.; Kepler, T.B.; Conolly, R.B. Quantitative evaluation of alternative mechanisms of blood and testes disposition of di(2-ethylhexyl) phthalate and mono(2-ethylhexyl) phthalate in rats. *Toxicol. Sci.* **1999**, *49*, 172–185. [CrossRef] [PubMed]

36. Koch, H.M.; Bolt, H.M.; Preuss, R.; Angerer, J. New metabolites of di(2-ethylhexyl)phthalate (DEHP) in human urine and serum after single oral doses of deuterium-labelled DEHP. *Arch Toxicol.* **2005**, *79*, 367–376. [CrossRef] [PubMed]

37. Adachi, K.; Suemizu, H.; Murayama, N.; Shimizu, M.; Yamazaki, H. Human biofluid concentrations of mono(2-ethylhexyl)phthalate extrapolated from pharmacokinetics in chimeric mice with humanized liver administered with di(2-ethylhexyl)phthalate and physiologically based pharmacokinetic modeling. *Environ. Toxicol. Pharmacol.* **2015**, *39*, 1067–1073. [CrossRef] [PubMed]

38. Choi, K.; Joo, H.; Campbell, J.L.; Andersen, M.E., Jr.; Clewell, H.J., 3rd. In vitro intestinal and hepatic metabolism of Di(2-ethylhexyl) phthalate (DEHP) in human and rat. *Toxicol. In Vitro* **2013**, *27*, 1451–1457. [CrossRef]

39. Weschler, C.J.; Nazaroff, W.W. Dermal Uptake of Organic Vapors Commonly Found in Indoor Air. *Environ. Sci. Technol.* **2014**, *48*, 1230–1237. [CrossRef]

40. Bu, Z.; Wang, J.; Yu, W.; Li, B. Dermal exposure to phthalates in home environment: Handwipes, influencing factors and implications. *Build. Environ.* **2018**, *133*, 1–7. [CrossRef]

41. Gong, M.; Zhang, Y.; Weschler, C.J. Predicting dermal absorption of gas-phase chemicals: Transient model development, evaluation, and application. *Indoor Air* **2014**, *24*, 292–306. [CrossRef]

42. Sui, H.-X.; Zhang, L.; Wu, P.-G.; Song, Y.; Yong, L.; Yang, D.-J.; Jiang, D.-G.; Liu, Z.-P. Concentration of di(2-ethylhexyl) phthalate (DEHP) in foods and its dietary exposure in China. *Int. J. Hyg. Environ. Health* **2014**, *217*, 695–701. [CrossRef] [PubMed]

43. Eveillard, A.; Lasserre, F.; De Tayrac, M.; Polizzi, A.; Claus, S.; Canlet, C.; Mselli-Lakhal, L.; Gotardi, G.; Paris, A.; Guillou, H. Identification of potential mechanisms of toxicity after di-(2-ethylhexyl)-phthalate (DEHP) adult exposure in the liver using a systems biology approach. *Toxicol. Appl. Pharmacol.* **2009**, *236*, 282–292. [CrossRef] [PubMed]

44. Yu, L.; Yang, M.; Cheng, M.; Fan, L.; Wang, X.; Xu, T.; Wang, B.; Chen, W. Associations between urinary phthalate metabolite concentrations and markers of liver injury in the US adult population. *Environ. Int.* **2021**, *155*, 106608. [CrossRef] [PubMed]

45. Erkekoğlu, P.; Rachidi, W.; De Rosa, V.; Giray, B.; Favier, A.; Hıncal, F. Protective effect of selenium supplementation on the genotoxicity of di(2-ethylhexyl)phthalate and mono(2-ethylhexyl)phthalate treatment in LNCaP cells. *Free Radic. Biol. Med.* **2010**, *49*, 559–566. [CrossRef] [PubMed]

46. Berger, K.; Eskenazi, B.; Balmes, J.; Holland, N.; Calafat, A.M.; Harley, K.G. Associations between prenatal maternal urinary concentrations of personal care product chemical biomarkers and childhood respiratory and allergic outcomes in the CHAMACOS study. *Environ. Int.* **2018**, *121*, 538–549. [CrossRef]

47. Huang, K.; He, Y.; Zhu, Z.; Guo, J.; Wang, G.; Deng, C.; Zhong, Z. Small, Traceable, Endosome-Disrupting, and Bioresponsive Click Nanogels Fabricated via Microfluidics for CD44-Targeted Cytoplasmic Delivery of Therapeutic Proteins. *ACS Appl. Mater. Interfaces* **2019**, *11*, 22171–22180. [CrossRef]